Supplementary Information

Materials. $Ni^{II}Cp(Ph_3P)Cl$, Zn dust were purchased from Aldrich and C_{60} of 99.98% purity from MTR Ltd. *o*-Dichlorobenzene ($C_6H_4Cl_2$) was distilled over CaH_2, P_2O_5 and K_2CO_3 under reduced pressure and hexane was distilled over Na/benzophenone. The solvents were degassed and stored in a glove box. All manipulations for the synthesis of **1** were carried out in a MBraun 150B-G glove box with controlled atmosphere and the content of H_2O and O_2 less than 1 ppm. The crystals were stored in the glove box and were sealed in 2 mm quarts tubes for EPR measurements under 10^{-3} Torr. KBr pellets for IR- and UV-visible-NIR measurements were prepared in the glove box.

Synthesis. Reduction of stoichiometric mixture of $Ni^{II}Cp(Ph_3P)Cl$ (18 mg, 0.042 mmol) and fullerene C_{60} (30 mg, 0.042 mmol) by excess of zinc dust (200 mg) in *o*-dichlorobenzene (16 ml) was carried out at 160°C during 10 minutes till the pink-red color of $Ni^{II}Cp(Ph_3P)Cl$ disappears and the violet color of starting C_{60} is distinguished. The reaction mixture was cooled to 100°C and stirred at this temperature for 4 hours. Solution was cooled to room temperature and stirred one more day to produce pale green solution. The solution was filtered in a glass tube of 46 ml volume and hexane (26 ml) was layered on the obtained solution. Slow diffusion of hexane during 1.5 months yielded crystals on the wall of the tube suitable for X-ray diffraction study using synchrotron radiation. Solvent was decanted from the crystals and they were washed with hexane to give small black plates of **1** with 46% yield. The composition of the crystals was determined by X-ray diffraction as $\{Ni(Ph_3P)\}_2(\mu_2\text{-}\eta^2, \eta2\text{-}C_{60})_2\cdot 2C_6H_4Cl_2$ (**1**).

General. UV-visible-NIR spectra were measured in KBr pellets on a Perkin Elmer Lambda 1050 spectrometer in the 250-2500 nm range. FT-IR spectra were obtained in KBr pellets with a Perkin-Elmer 1000 Series spectrometer (400-7800 cm^{-1}). EPR spectra were recorded for a polycrystalline sample at room temperature with a JEOL JES-TE 200 X-band ESR spectrometer.

Computational details

Density functional theory (DFT) calculations by B3LYP, [1] CAM-B3LYP,[2] and ωB97X-D[3] and time-dependent DFT (TD-DFT) by CAM-B3LYP were carried out based on X-ray structure of $\{Ni(Ph_3P)\}_2(C_{60})_2$ dimer in major position. Disordered dichlorobenzene molecule was not included in the present calculations. B3LYP is a widely used hybrid functional which contains 20% Hartree–Fock (HF) exchange. CAM-B3LYP includes 19% HF exchange at short range and 65% HF exchange at long range, whereas ωB97X-D includes 22% HF exchange at short range and 100% HF exchange at long range and also corrected by empirical dispersion[4]. The double-ζ basis set with effective core potential (LanL2DZ[5]) for nickel atoms, the double-ζ basis set with polarization functions of d-type on heavy atoms and p-type on hydrogen (6-31G(d,p)[6]) were used. The stability of singlet and triplet wave functions were confirmed by specifying the "Stable=Opt" keyword in the present DFT calculations. All computations were performed with the Gaussian 09 program package[7].

Crystal data for {Ni(PPh$_3$)}$_2$(C$_{60}$)$_2$·2C$_6$H$_4$Cl$_2$ (1). Data collection for the crystals of **1** was carried out at 100 K with a MAR225 CCD detector using synchrotron radiation (λ = 0.87933 Å) at the BESSY storage ring, BL 14.2 (PSF of the Free University of Berlin, Germany). The structure was solved by direct method and refined by the full-matrix least-squares method against F^2 using SHELX-97 package[8]. Non-hydrogen atoms were refined in the anisotropic approximation. Positions of hydrogen atoms for phenyl groups were calculated geometrically and refinedin the riding mode. The Ni(Ph$_3$P) fragment is disordered between two positions having 0.936/0.064(2) occupancies. For minor position only Ni and P atoms were included into refinement, whereas the contribution of disordered phenyl groups has been neglected due to low occupancy. The solvent $C_6H_4Cl_2$ molecule is disordered between two orientations with the 0.595/0.405(3) occupancies. Most probably, the minor orientation of the Ni(Ph$_3$P) fragment is accompanied by an alternative location of *o*-diclorobenezene on the site of the major orientation of Ni(Ph$_3$P), thus retaining the stoichiometric 1:2 composition of the solvated complex.

References

(1) K. Ragavachari, *Theor. Chem. Acc.* **2000**, *103*, 361 and references cited therein.

(2) a) T. Yanai, D. Tew, N. Handy, *Chem. Phys. Lett.* **2004**, *393*, 51; b) M. J. G. Peach, P. Benfield, T.; Helgaker, D. J. Tozer, *J. Chem. Phys.* **2008**, *128*, 044118.

(3) J. -Da. Chai, M. Head-Gordon, *Phys. Chem. Chem. Phys.* **2008**, *10*, 6615.

(4) S. Grimme, *J. Comput. Chem.* **2008**, *27*, 1787.

(5) a) P. J. Hay, W. R. Wadt, *J. Chem. Phys.* **1985**, *82*, 270; b) W. R. Wadt, P. J. Hay, *J. Chem. Phys.* **1985**, *82*, 284; c) P. J. Hay, W. R. Wadt, *J. Chem. Phys.* **1985**, *82*, 299.

(6) a) Hehre W. J., R. Ditchfield, J. A. Pople, *J. Chem. Phys.* **1972**, *56*, 2257; b) P. C. Hariharan, J. A. Pople, *Mol. Phys.* **1974**, *27*, 209; c) P. C. Hariharan, J. A. Pople, *Theo. Chim. Acta* **1973**, *28*, 213; d) M. M.; Francl, W. J., Pietro Hehre, W. J. Binkley, J.S. Gordon, M. S. DeFrees, D. J. J. A. Pople, *J. Chem. Phys.* **1982**, *77*, 3654.

(7) Gaussian 09, Revision D.01, M. J. Frisch, G. W. Trucks, H. B. Schlegel, G. E. Scuseria, M. A. Robb, J. R. Cheeseman, G. Scalmani, V. Barone, B. Mennucci, G. A. Petersson, H. Nakatsuji, M. Caricato, X. Li, H. P. Hratchian, A. F. Izmaylov, J. Bloino, G. Zheng, J. L. Sonnenberg, M. Hada, M. Ehara, K. Toyota, R. Fukuda, J. Hasegawa, M. Ishida, T. Nakajima, Y. Honda, O. Kitao, H. Nakai, T. Vreven, J. A. Montgomery, Jr., J. E. Peralta, F. Ogliaro, M. Bearpark, J. J. Heyd, E. Brothers, K. N. Kudin, V. N. Staroverov, R. Kobayashi, J. Normand, K. Raghavachari, A. Rendell, J. C. Burant, S. S. Iyengar, J. Tomasi, M. Cossi, N. Rega, J. M. Millam, M. Klene, J. E. Knox, J. B. Cross, V. Bakken, C. Adamo, J. Jaramillo, R. Gomperts, R. E. Stratmann, O. Yazyev, A. J. Austin, R. Cammi, C. Pomelli, J. W. Ochterski, R. L. Martin, K. Morokuma, V. G. Zakrzewski, G. A. Voth, P. Salvador, J. J. Dannenberg, S. Dapprich, A. D. Daniels, Ö. Farkas, J. B. Foresman, J. V. Ortiz, J. Cioslowski, and D. J. Fox, Gaussian, Inc., Wallingford CT, 2013.

(8) G.M. Sheldrick, *Acta Cryst A*, **2008**, *64*, 112.

Table S1. IR spectra of parent compounds and **1**.

	Components			**1**
	C_{60}	**$Ni^{II}Cp(Ph_3P)Cl$**	**$C_6H_4Cl_2$**	
C_{60}	526s			525s
	576m			578w
	1182w			1183w
	1429s			1420m
$Ni(Ph_3P)$		438w		-
		452w		-
		499m		490w
		510m		-
		532s		538m
		693m		692s
		703m		721m
		749m		746s*
		-		810w
		833w		835w
		998w		997w
		1094w		1096w
		1159w		1158w
		1185w		1183w
		1434s		1433s
		1480w		1481w
		-		1570w
$C_6H_4Cl_2$			657w	657w
			748s	746s*
			1030m	1033w
			1122m	1118m
			1453m	1455s

w- weak, m- middle, s- strong intensity; * bands are coincided.

Spectrum of 1 in the UV-visible-NIR range.

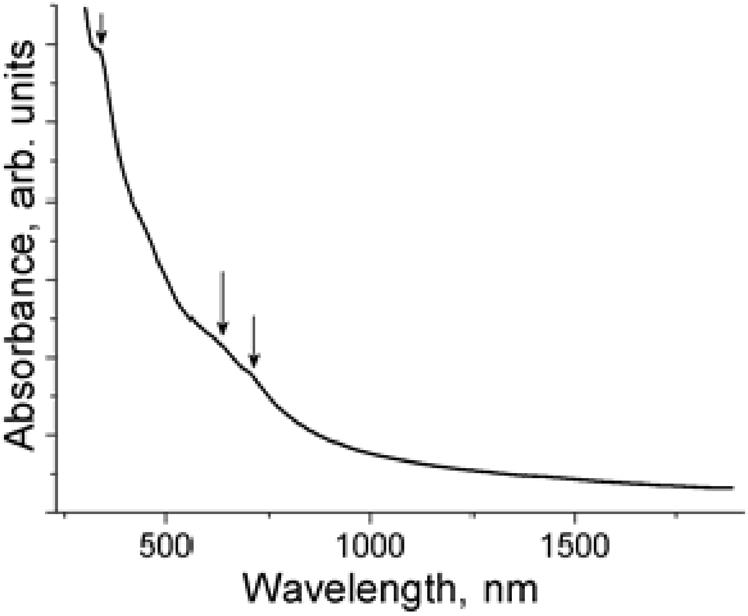

Figure S1. Spectrum of **1** in KBr pellet prepared in anaerobic condition in the 300-1800 nm range. Bands are marked by arrows.

Crystal structure of 1.

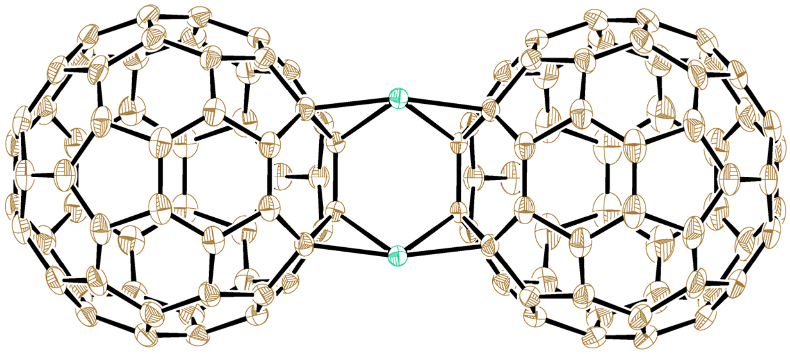

Figure S2. Molecular structure of **1** viewed perpendicular to the Ni···Ni line without Ph_3P ligands. Carbon atoms are indicated in brown, nickel atoms are green, and phosphorus atoms are orange. Solvent molecules are not shown for clarity.

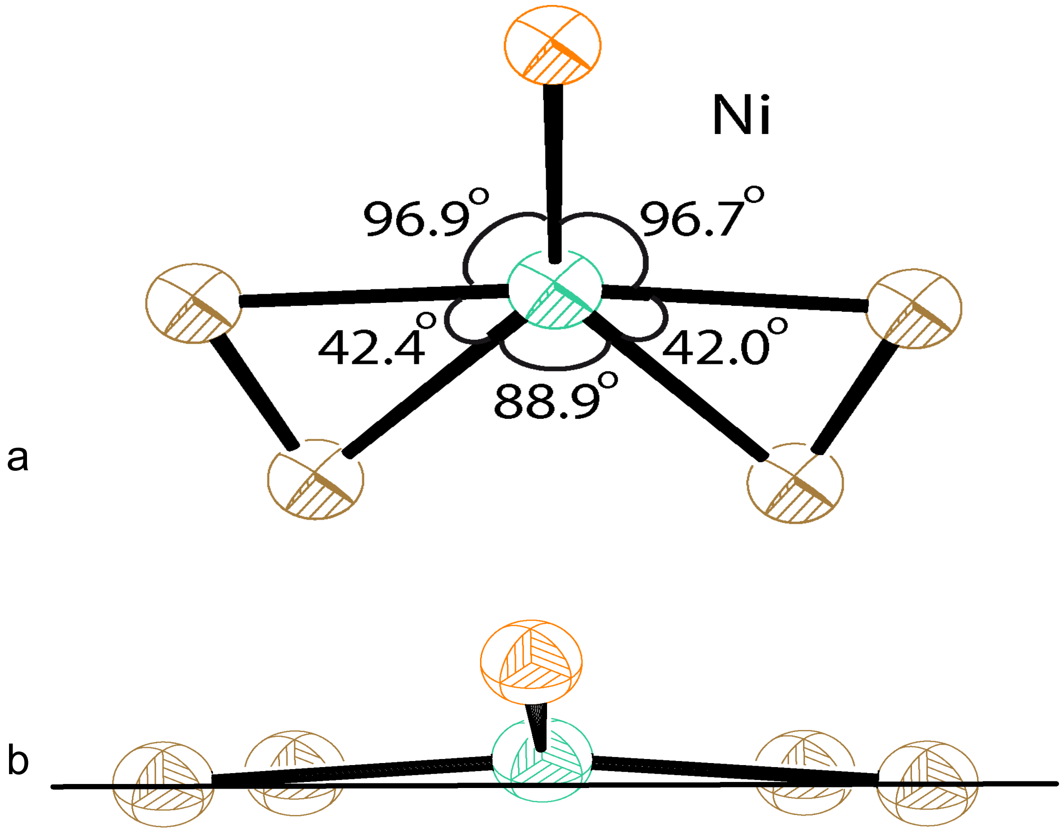

Figure S3. The surrounding of nickel atom from four carbon and phosphorus atoms, viewed from the direction perpendicular to the C_4 plane (a) and along this plane (b).

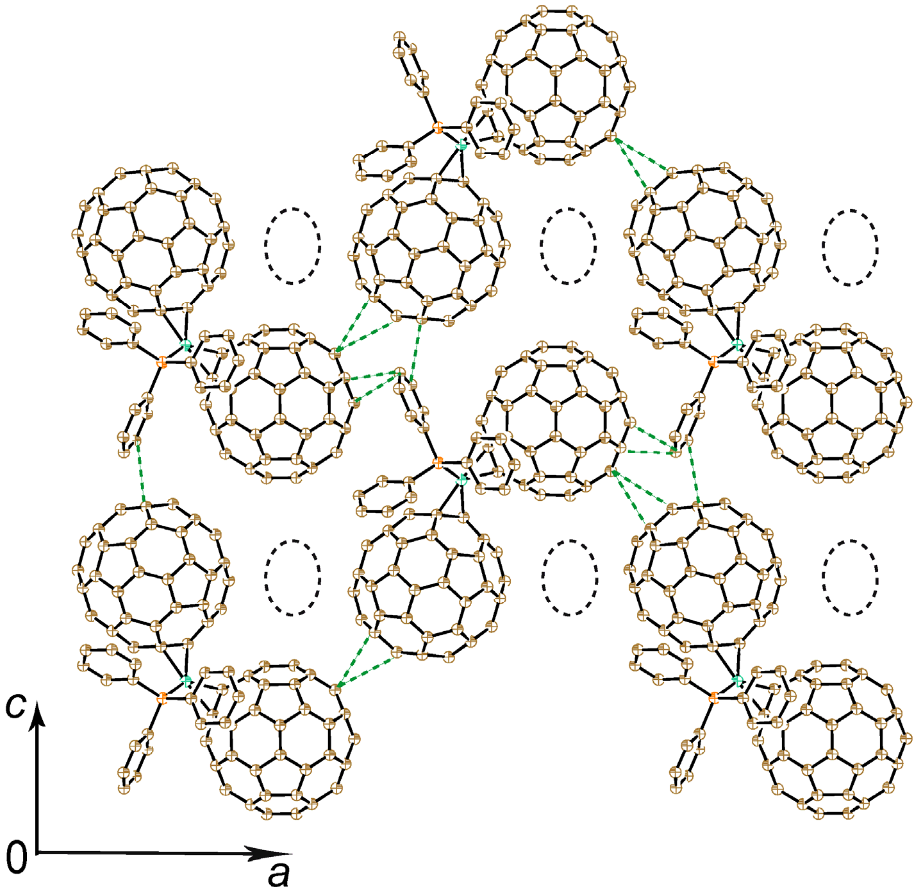

Figure S4. View on crystal structure of **1** along the *b*-axis. Only major orientation of Ni(Ph_3P) fragment is shown. Short van der Waals C…C contacts are shown by green dashed lines. Dashed ovals indicate positions occupied by disordered solvent $C_6H_4Cl_2$ molecules.

DFT calculations.

Table S2. Total and relative energies (E and E_{rel}) and $<S^2>$ values for the singlet and triplet states of $\{\mathrm{Ni(Ph_3P)}\}_2(\mathrm{C_{60}})_2$ dimer[a] calculated at the B3LYP, CAM-B3LYP, and ωB97X-D/LanL2DZ/6-31G(d,p) levels of theory.

Method	State	E/ hartree	E_{rel}/ K	$<S^2>$
RB3LYP	$^1A'$	−6983.0820	0	0
UB3LYP	$^3A''$	−6983.0215	19105.16	2.046
RCAM-B3LYP	$^1A'$	−6979.6612	0	0
UCAM-B3LYP	$^3A''$	−6979.5827	24791.54	2.064
RωB97X-D	$^1A'$	−6981.3181	0	0
UωB97X-D	$^3A''$	−6981.2361	25899.72	2.068

[a]The dimer has the C_S symmetry.

Table S3. Calculated charges of $\{\mathrm{Ni(Ph_3P)}\}_2(\mathrm{C_{60}})_2$ dimer at the ground state by Mulliken and natural population analyses (NPA) at the B3LYP, CAM-B3LYP, and ωB97X-D/LanL2DZ/6-31G(d,p) levels of theory.

	RB3LYP		RCAM-B3LYP		RωB97X-D	
	Mulliken	NPA	Mulliken	NPA	Mulliken	NPA
Ni	−0.121	+0.226	−0.187	+0.222	−0.077	+0.224
C_{60}(A)	−0.322	−0.583	−0.277	−0.569	−0.358	−0.570
C_{60}(B)	−0.270	−0.551	−0.222	−0.535	−0.303	−0.537
TPP	+0.417	+0.341	+0.436	+0.329	+0.407	+0.330

Table S4. Excitation energies (Δ*E*), oscillator strengths (*f*), assignments, and charges of Ni, C_{60}, Ph_3P molecules by natural population analysis (NPA) in the ground (S_0) and low-lying excited (S_n, n = 1-6) states for $\{Ni(Ph_3P)\}_2(C_{60})_2$ dimer calculated at the TD-RCAM-B3LYP/LanL2DZ/6-31G(d,p) level of theory.

State	Δ*E*/ eV	*f*	Assignment	NPA charge Ni/C60(A)/C60(B)/Ph_3P
S_0				+0.222/−0.569/−0.535/+0.329
S_1	2.330	0.0019	HO→LU(43%) HO−2→LU(21%) HO−2→LU+1(15%) HO−4→LU(6%) HO−7→LU(2%)	+0.230/−0.559/−0.602/+0.350
S_2	2.347	0.0005	HO→LU+1(48%) HO−2→LU(25%) HO−2→LU+1(9%) HO−9→LU+1(4%) HO→LU(4%)	+0.231/−0.638/−0.514/+0.345
S_3	2.367	0.0001	HO−4→LU(65%) HO−4→LU+1(18%) HO−2→LU(5%) HO→LU(2%) HO−4→LU+3(2%)	+0.223/−0.564/−0.542/+0.330
S_4	2.374	0.0022	HO−1→LU(42%) HO−3→LU(24%) HO−3→LU+1(17%) HO−6→LU(6%)	+0.227/−0.554/−0.571/+0.335
S_5	2.404	0.0015	HO−1→LU+1(43%) HO−3→LU(23%) HO−3→LU+1(12%) HO→LU+2(4%) HO−1→LU(4%) HO−6→LU+1(3%)	+0.229/−0.605/−0.523/+0.335
S_6	2.484	0.0000	HO−5→LU+1(63%) HO−5→LU(21%) HO−2→LU+1(3%) HO−5→LU+3(3%)	+0.223/−0.572/−0.534/+0.330

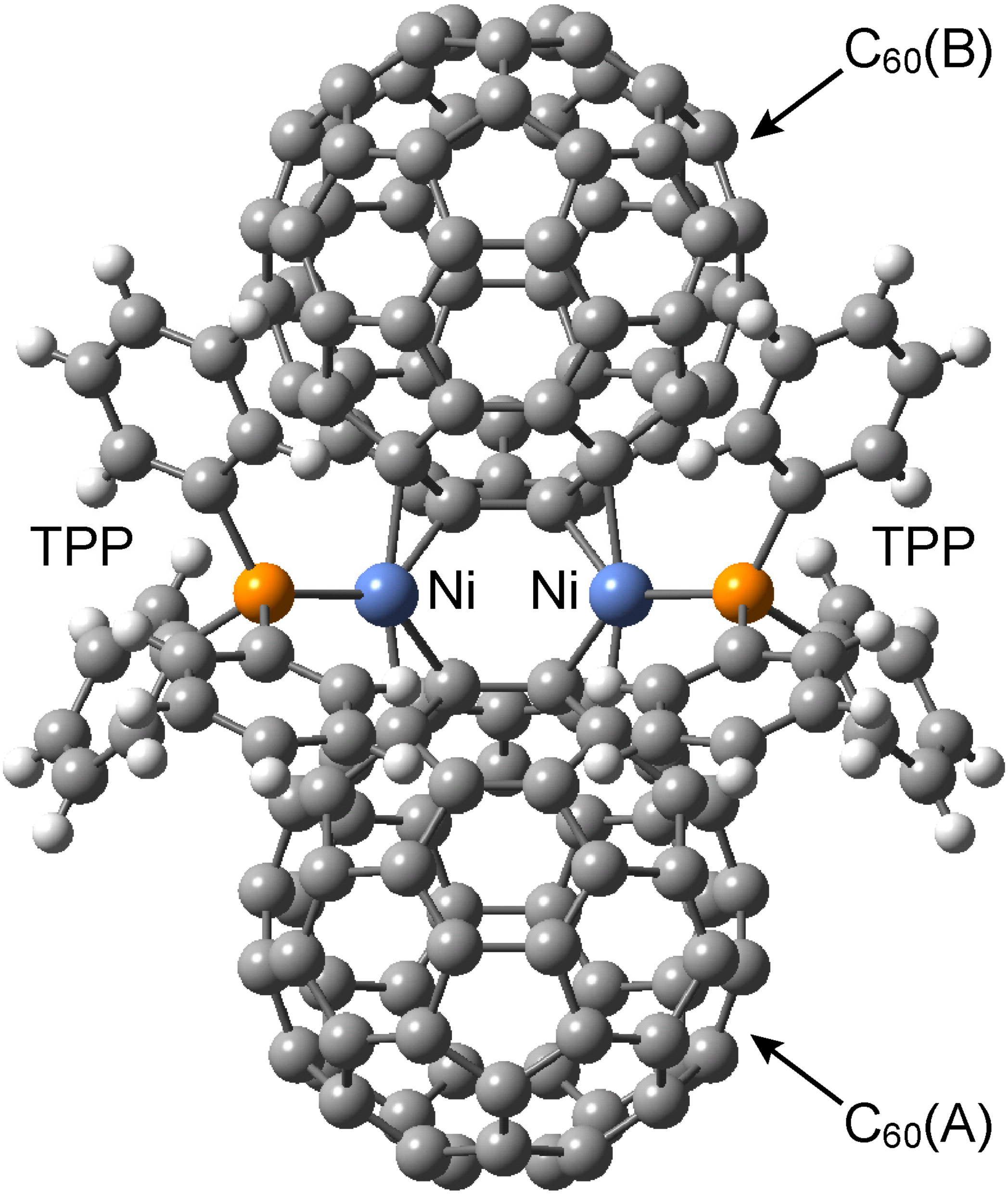

Figure S5. The unit of $\{Ni(Ph_3P)\}_2(C_{60})_2$ dimer for the calculations, which shows a C_S symmetry.

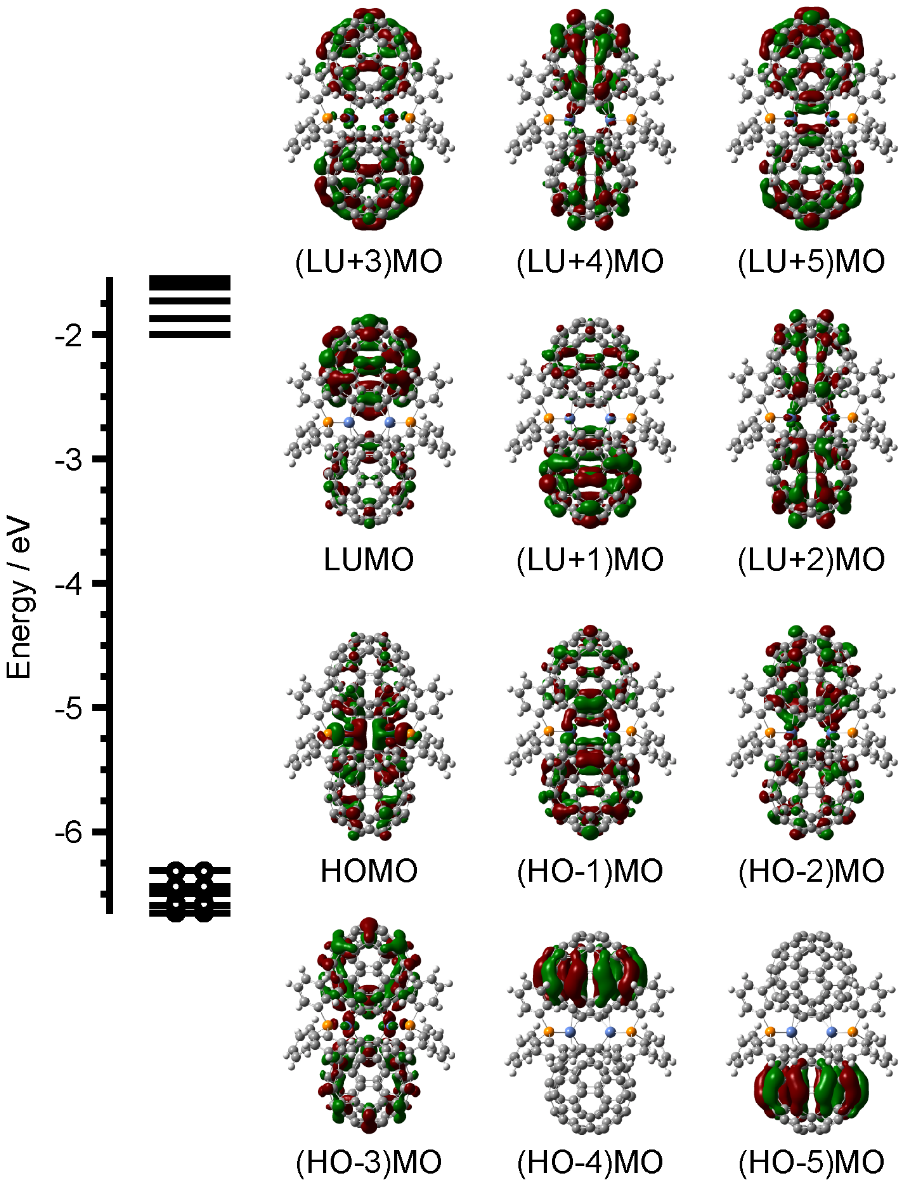

Figure S6. Energy diagram of frontier orbitals for the $^1A'$ state of the $\{Ni(Ph_3P)\}_2(C_{60})_2$ dimer calculated at the RCAM-B3LYP/LanL2DZ/6-31G(d,p) level of theory.

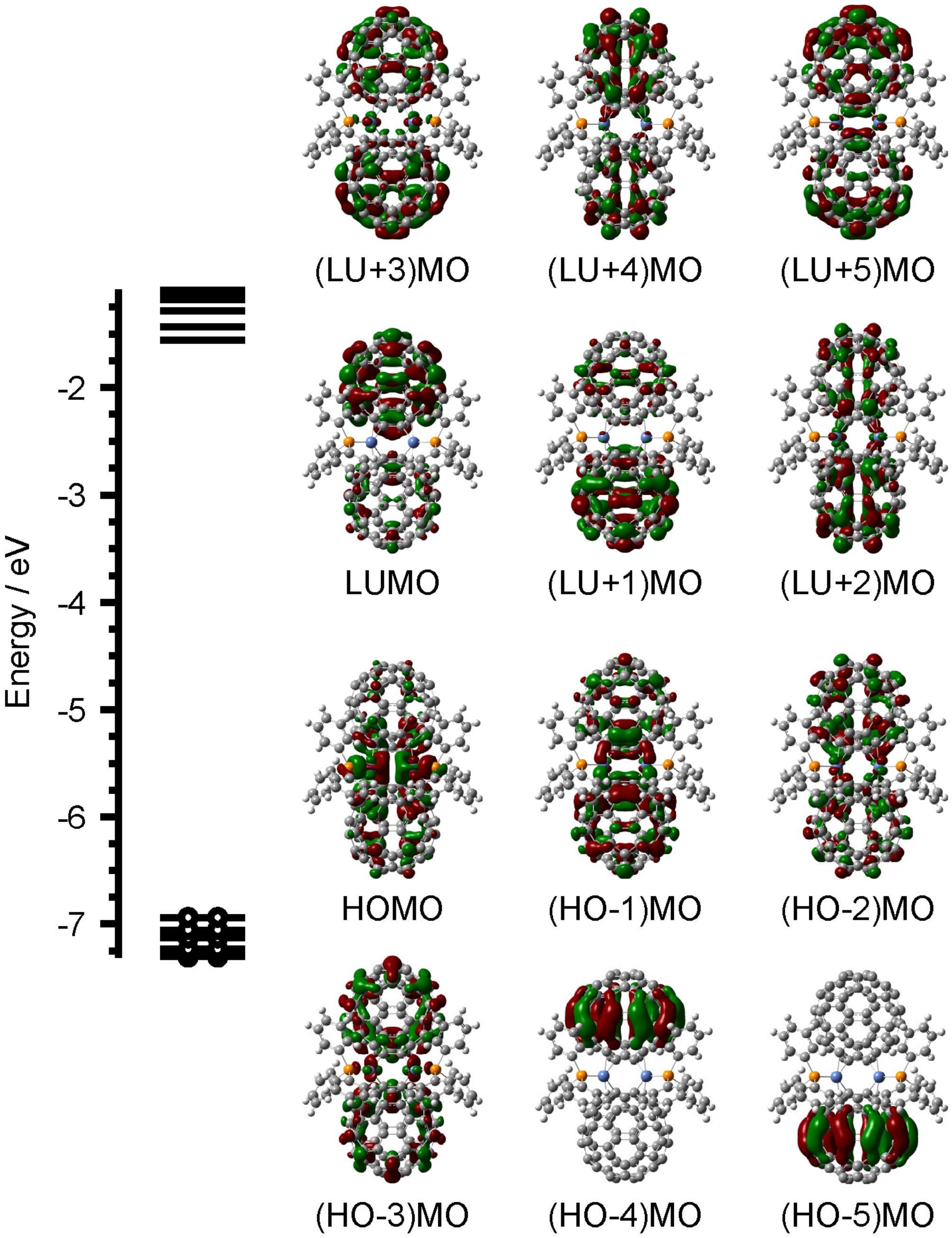

Figure S7. Energy diagram of frontier orbitals for the $^{1}A'$ state of the $\{Ni(Ph_3P)\}_2(C_{60})_2$ dimer calculated at the RωB97X-D/LanL2DZ/6-31G(d,p) level of theory.